

Neutral-pH Overall Water Splitting Catalyzed Efficiently by a Hollow and Porous Structured Ternary Nickel Sulfoselenide Electrocatalyst

Lingyou Zeng, Kaian Sun, Yanju Chen, Zhi Liu, Yinjuan Chen, Yuan Pan, Ruiyu Zhao,
Yunqi Liu* and Chenguang Liu*

State Key Laboratory of Heavy Oil Processing, Key Laboratory of Catalysis, China University
of Petroleum (East China), Qingdao, 266580, P. R. China.

Corresponding Author: *E-mail: panyuan@upc.edu.cn; liuyq-group@upc.edu.cn (Y. L.)

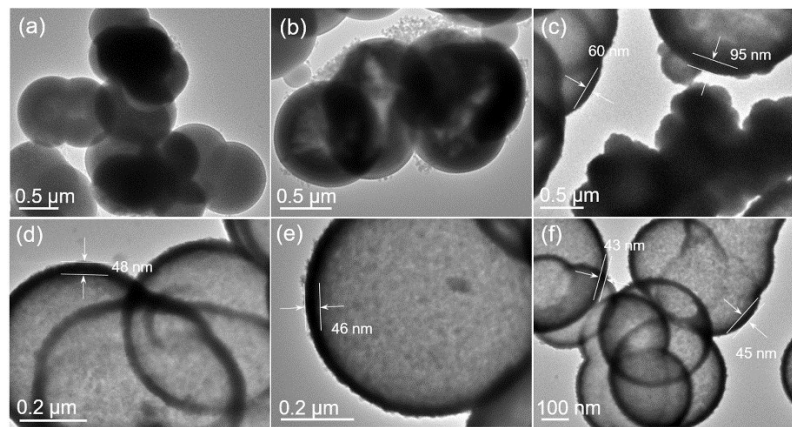


Figure S1. TEM images of the time-dependent formation of hollow NiS₂ spheres. (a) 1 h; (b) 2 h; (c) 4 h; (d) 12 h; (e) 24 h; (f) 36 h. The wall thicknesses of hollow spheres were measured and marked in the images. Figure S1 shows that the NiS₂ solid spheres entirely transform into hollow spheres when the hydrothermal time reaches to 12 h. When continue to extend the hydrothermal time from 12 h to 36 h, the wall thicknesses of hollow spheres slightly decrease from 48 nm to 43 nm.

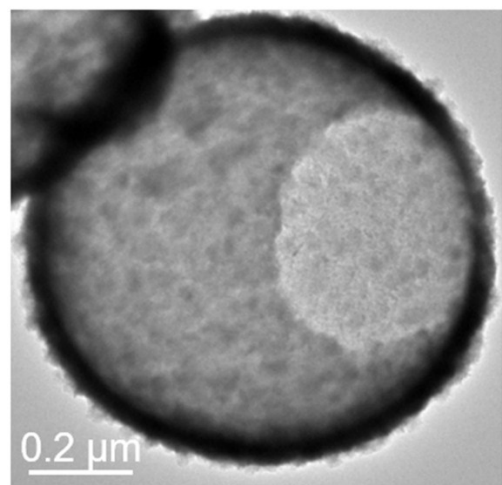


Figure S2. TEM image of a typical hollow NiS_2 microsphere with a broken shell.

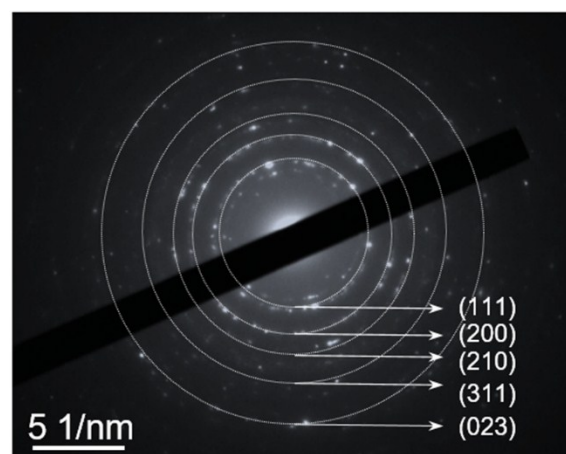


Figure S3. The selective area electron diffraction (SAED) pattern of the $\text{Ni}(\text{S}_{0.5}\text{Se}_{0.5})_2$ electrocatalyst.

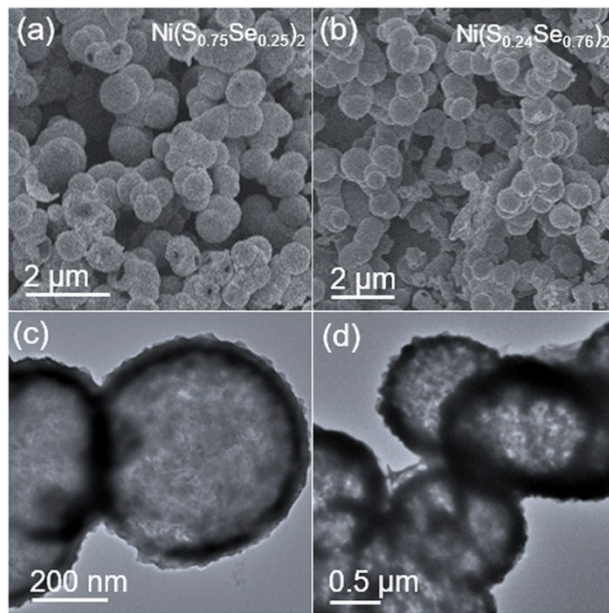


Figure S4. (a, b) SEM and (c, d) TEM images of the $\text{NiS}_{2(1-x)}\text{Se}_{2x}$ porous/hollow spheres with (a, c) $x = 0.25$ and (b, d) $x = 0.72$.

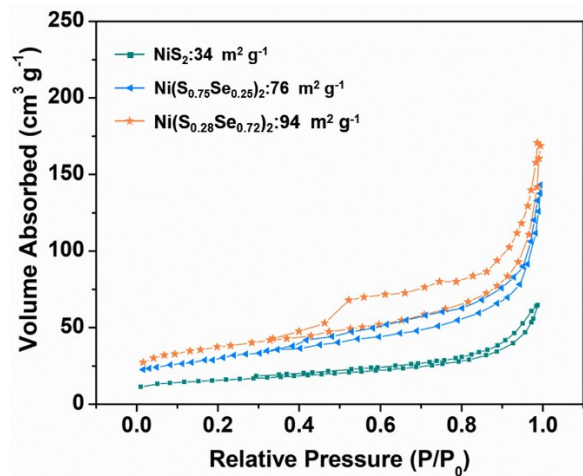


Figure S5. Nitrogen sorption isotherms of NiS_2 , $\text{Ni}(\text{S}_{0.75}\text{Se}_{0.25})_2$ and $\text{Ni}(\text{S}_{0.28}\text{Se}_{0.72})_2$ samples.

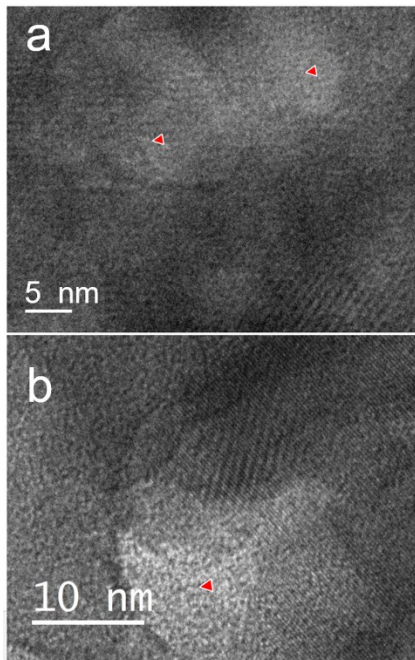


Figure S6. HRTEM images of the $\text{Ni}(\text{S}_{0.5}\text{Se}_{0.5})_2$ catalyst. Red arrows refer to porous structure.

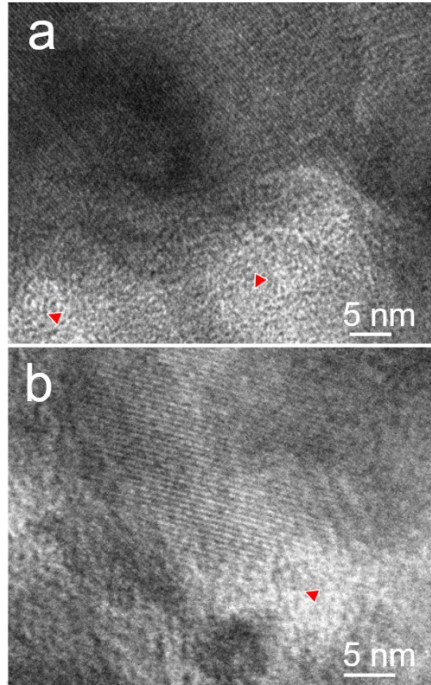


Figure S7. HRTEM images of (a) $\text{Ni}(\text{S}_{0.75}\text{Se}_{0.25})_2$ and (b) $\text{Ni}(\text{S}_{0.28}\text{Se}_{0.72})_2$ catalysts. Red arrows refer to porous structure.

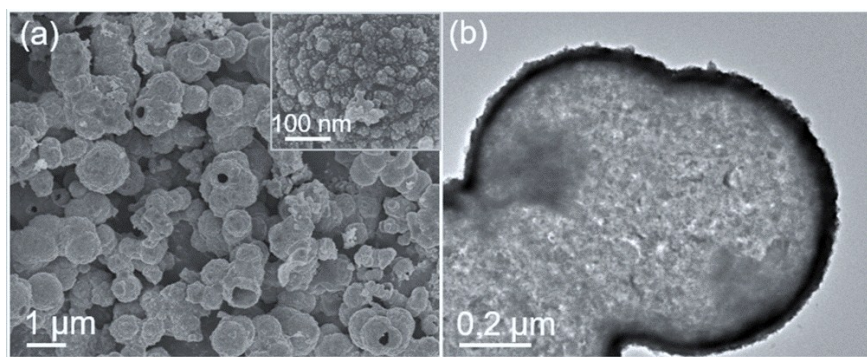


Figure S8. SEM images (a) and TEM image (b) for $\text{Ni}(\text{S}_{0.5}\text{Se}_{0.5})_2$ catalyst after long-term stability test.

Table S1. Chemical composition and electrocatalytic performance of the porous/hollow NiS_{2(1-x)Se_{2x}} catalysts.

		NiS ₂	Ni(S _{0.75} Se _{0.25}) ₂	Ni(S _{0.5} Se _{0.5}) ₂	Ni(S _{0.28} Se _{0.72}) ₂
selenization process	feed mass ratio ^{a)}	—	1:2	1:5	1:10
	reaction time (h)	—	2	2	5
S:Se ratio from ICP		—	0.745:0.253	0.494:0.506	0.282:0.718
η_{10} ^{b)} (mV)	HER	245	171	124	141
	OER	665	595	501	540
Tafel slope (mV dec ⁻¹)	HER	106	86	81	92
	OER	182	105	94	121
C _{dl} (mF cm ⁻²)		4.6	8.7	12.9	9.8
C _{dl} -normalized activity ^{c)}		0.41	0.74	1.55	1.32
BET surface area (m ² g ⁻¹)		34	76	91	94
BET-normalized activity ^{d)}		0.04	0.09	0.22	0.13

a) feed mass ratio: mass ratio of NiS₂ to Se powder (g/g). b) η_{10} : overpotential requirement for current density of 10 mA cm⁻². c) and d) : HER current densities at -150 mV vs. RHE normalized to C_{dl} and BET surface area, respectively.

Table S2. Comparison of the HER performance of $\text{Ni}(\text{S}_{0.5}\text{Se}_{0.5})_2$ with other earth-abundant HER electrocatalysts in neutral electrolyte.

Catalysts	Support	Mass loading (mg cm ⁻²)	η vs. RHE (mV) @j=10 mA cm ⁻²	Tafel slope (mV dec ⁻¹)	Electrolyte	Reference
$\text{Ni}(\text{S}_{0.5}\text{Se}_{0.5})_2$	Ni foam	0.75	124	81	1 M PBS	This work
CoP nanowire/CC	Carbon cloth	0.92	106	93	1 M PBS	[1]
MoP/CFP	Carbon paper	2.8	165	105	1 M PBS	[2]
MoS_2/Ti plate	Ti plate	1.5	200	152	1 M PBS	[3]
FeP NAs	Glass carbon	N.A.	202	71	1 M PBS	[4]
CoP NS	Ti plate	2.0	149	58	1 M PBS	[5]
$\text{Ni}_{0.1}\text{Co}_{0.9}\text{P}$	Carbon paper	0.58	125	103	1 M PBS	[6]
Ni-doped FeP/C	Carbon paper	0.4	117	81	1 M PBS	[7]
Amorphous Co-S film	FTO	1.5	160	93	1 M PBS	[8]
Co-C-N complex	Glass carbon	1.25	107	273	1 M PBS	[9]
CoP-MNA/NF	Ni foam	0.92	189	180	0.5 M PBS	[10]
3D $\text{MoS}_2/\text{N-GAs}$	Glass carbon	0.7	261	230	1 M PBS	[11]

Table S3. Comparison of the OER performance of $\text{Ni}(\text{S}_{0.5}\text{Se}_{0.5})_2$ with other earth-abundant OER electrocatalysts in neutral electrolyte.

Catalysts	Support	Mass loading (mg cm ⁻²)	η vs. RHE (mV) @j=10 mA cm ⁻²	Tafel slope (mV dec ⁻¹)	Electrolyte	Ref.
$\text{Ni}(\text{S}_{0.5}\text{Se}_{0.5})_2$	Ni foam	0.75	501	94	1 M PBS (pH 7)	This work
Co_3S_4 ultrathin nanosheets	Glassy carbon	N.A.	700	151	PBS (pH 7)	[12]
a-Co ₂ P	Glassy carbon	N.A.	592	94.4	0.1 M PBS	[13]
1-D CoHCF	Glass substrate	1.0	880	N.A.	PBS (pH 7)	[14]
Co-Bi NS/G	Glass carbon	0.285	570 mV @ 14.4	160	PBS (pH 7)	[15]
Bi_2WO_6 CNPs	Glass carbon	0.34	540	N.A.	0.5 M Na_2SO_4 (pH 6.6)	[16]
$\text{CuCo}_2\text{O}_4/\text{NrGO}$	Glass carbon	0.8	540	79	0.1 M PBS (pH 7.6)	[17]

N.A. stands for not given.

Table S4. Comparison of recent bifunctional electrocatalysts for overall water splitting in neutral electrolytes.

Catalysts	Support	Mass loading (mg cm ⁻²)	Electrolyte	HER η_{10} (mV)	HER Tafel slope (mV dec ⁻¹)	OER η_{10} (mV)	OER Tafel slope (mV dec ⁻¹)	E ₁₀ (V)	Ref.
Ni(S _{0.5} Se _{0.5}) ₂	Ni foam	0.75	1 M PBS (pH 7)	124	81	501	94	1.87	This work
S-NiFe ₂ O ₄	Ni foam	N.A.	1 M PBS (pH 7)	197	81.3	494	118.1	1.95	[18]
CoO/CoSe ₂ -Ti	Ti mesh	2.0	0.5 M PBS	337	131	510	137	2.18	[19]
Ni _{0.1} Co _{0.9} P	Carbon paper	0.58	1 M PBS (pH 7)	125	103	570	133	1.89	[6]

N.A. stands for not given.

References

- [1] J. Tian, Q. Liu, A. M. Asiri, X. Sun, *J. Am. Chem. Soc.* **2014**, 136, 7587.
- [2] X. Zhang, F. Zhou, W. Pan, Y. Liang, R. Wang, *Adv. Funct. Mater.* **2018**, 28, 1804600.
- [3] J. Shi, J. Hu, *Electrochim. Acta* **2015**, 168, 256.
- [4] Y. Liang, Q. Liu, A. M. Asiri, X. Sun, Y. Luo, *J. Am. Chem. Soc.* **2013**, 135, 17699.
- [5] Z. Pu, Q. Liu, P. Jiang, A. M. Asiri, A. Y. Obaid, X. Sun, *Chem. Mater.* **2014**, 26, 4326.
- [6] R. Wu, B. Xiao, Q. Gao, Y.-R. Zheng, X.-S. Zheng, J.-F. Zhu, *Angew. Chem. Int. Ed.* **2018**, 57, 15445.
- [7] F. L. Xue, L. Yu, X. W. D. Lou, *Sci. Adv.* **2019**, 5, eaav6009.
- [8] Y. Sun, C. Liu, D. C. Grauer, J. Yano, J. R. Long, P. Yang, C. J. Chang, *J. Am. Chem. Soc.* **2013**, 135, 17699.
- [9] Z.-L. Wang, X.-F. Hao, Z. Jiang, X.-P. Sun, D. Xu, J. Wang, H.-X. Zhong, F.-L. Meng, X.-B. Zhang, *J. Am. Chem. Soc.* **2015**, 137, 15070.
- [10] Y. P. Zhu, Y. P. Liu, T. Z. Ren, Z. Y. Yuan, *Adv. Funct. Mater.* **2015**, 25, 7337.
- [11] Y. Hou, B. Zhang, Z. Wen, S. Cui, X. Guo, Z. He, J. Chen, *J. Mater. Chem. A* **2014**, 2, 13795.
- [12] Y. Liu, C. Xiao, M. Lyu, Y. Lin, W. Cai, P. Huang, W. Tong, Y. Zou, Y. Xie, *Angew. Chem. Int. Ed.* **2015**, 54, 11231.
- [13] K. Xu, H. Cheng, L. Liu, H. Lv, X. Wu, C. Wu, Y. Xie, *Nano Lett.* **2017**, 17, 578.
- [14] H. T. Bui, N. K. Shrestha, M. M. Sung, J. K. Lee, S.-H. Han, *J. Mater. Chem. A* **2016**, 4, 9781.
- [15] P. Chen, K. Xu, T. Zhou, Y. Tong, J. Wu, H. Cheng, X. Lu, H. Ding, C. Wu, Y. Xie, *Angew. Chem. Int. Ed.* **2016**, 55, 2488.
- [16] Z.-P. Nie, D.-K. Ma, G.-Y. Fang, W. Chen, S.-M. Huang, *J. Mater. Chem. A* **2016**, 4, 2438.
- [17] L. Xie, R. Zhang, L. Cui, D. Liu, S. Hao, Y. Ma, G. Du, A. M. Asiri, X. Sun, *Angew. Chem. Int. Ed.* **2017**, 56, 1064.
- [18] J. Liu, D. Zhu, T. Ling, A. Vasileff, S.-Z. Qiao, *Nano Energy* **2017**, 40, 264.
- [19] K. Li, J. Zhang, R. Wu, Y. Yu, B. Zhang, *Adv. Sci.* **2016**, 3, 1500426.